

# First experience with single-source, dual-energy CCTA for monochromatic stent imaging

Julia Stehli<sup>1†</sup>, Tobias A. Fuchs<sup>1†</sup>, Adrian Singer<sup>1</sup>, Sacha Bull<sup>1</sup>, Olivier F. Clerc<sup>1</sup>, Mathias Possner<sup>1</sup>, Oliver Gaemperli<sup>1,2</sup>, Ronny R. Buechel<sup>1</sup>, and Philipp A. Kaufmann<sup>1\*</sup>

<sup>1</sup>Department of Nuclear Medicine, Cardiac Imaging, University Hospital Zurich, CH-8091 Zurich, Switzerland; and <sup>2</sup>Department of Cardiology, University Hospital Zurich, Ramistrasse 100, NUK C 42, CH-8091 Zurich, Switzerland

Received 16 April 2014; accepted after revision 11 November 2014; online publish-ahead-of-print 18 December 2014

## Aims

Single-source, dual-energy coronary computed tomography angiography (CCTA) with monochromatic image reconstruction allows significant noise reduction. The aim of the study was to evaluate the impact of monochromatic CCTA image reconstruction on coronary stent imaging, as the latter is known to be affected by artefacts from highly attenuating strut material resulting in artificial luminal narrowing.

## Methods and results

Twenty-one patients with 62 stents underwent invasive coronary angiography and single-source, dual-energy CCTA after stent implantation. Standard polychromatic images as well as eight monochromatic series (50, 60, 70, 80, 90, 100, 120, and 140 keV) were reconstructed for each CCTA. Signal and noise were measured within the stent lumen and in the aortic root. Mean in-stent luminal diameter was assessed in all CCTA reconstructions and compared with quantitative invasive coronary angiography (QCA). Luminal attenuation was higher in the stent than in the aortic root throughout all monochromatic reconstructions ( $P < 0.001$ ). An increase in monochromatic energy was associated with a decrease in luminal attenuation values ( $P < 0.001$ ). The mean in-stent luminal diameter underestimation by monochromatic CCTA compared with QCA was 90% at low monochromatic energy (50 keV) and improved to 37% at high monochromatic (140 keV) reconstruction while stent diameter was underestimated by 39% with standard CCTA.

## Conclusion

Monochromatic CCTA can be used reliably in patients with coronary stents. However, reconstructions with energies below 80 keV are not recommended as the blooming artefacts are most pronounced at such low energies, resulting in up to 90% stent diameter underestimation.

## Keywords

Gemstone Spectral Imaging • single-source dual-energy CCTA • stent imaging

## Introduction

Coronary computed tomography angiography (CCTA) in native coronary arteries is widely accepted as diagnostic and prognostic tool for coronary artery disease (CAD) evaluation.<sup>1,2</sup> Its clinical use for stent imaging remains controversial because of beam hardening causing 'blooming' artefacts induced by partial volume artefacts from highly attenuated stent struts,<sup>3–5</sup> resulting in artificial luminal narrowing.<sup>6</sup> This causes an underestimation of the true luminal diameter, which leads to a rather low positive predictive value in the detection of in-stent restenosis.<sup>7–9</sup> This is of importance as 5–10% of coronary stents develop in-stent restenosis,<sup>10</sup> despite the introduction of drug-eluting stents and latest guidelines on coronary

revascularization specifically recommend a follow-up CCTA for patients with unprotected left main stenting.<sup>11</sup>

Recently, a new CT technology, combining single-source, dual-energy CT with latest gemstone detectors for spectral imaging (GSI) was introduced.<sup>12</sup> The technology is integrated into a 64-slice, high-definition CT (HDCT) scanner (Discovery CT 750 High Definition, GE Healthcare, Milwaukee, WI, USA), which is equipped with a source that can switch energy rapidly<sup>13</sup> and hence creates two data sets obtained from the two different energies acquired in virtually the same tube angle. These data sets can be used to synthesize monochromatic images, which mimic images as if different monochromatic x-ray sources were used. A recent study showed that GSI with monochromatic reconstructions offers significant noise

\* Corresponding author. Tel: +41 44 255 41 96; Fax: +41 44 255 44 14, E-mail: pak@usz.ch

† These authors contributed equally to this work.

Published on behalf of the European Society of Cardiology. All rights reserved. © The Author 2014. For permissions please email: journals.permissions@oup.com.

reduction and image quality improvement<sup>14</sup> and may offer further benefits.<sup>15</sup> The aim of the study was to evaluate the impact of monochromatic CCTA image reconstruction on coronary stent imaging.

## Methods

### Study population

Twenty-one patients with known CAD and previous stent implantation who were referred by clinical indication for percutaneous coronary intervention (PCI) underwent a prospectively triggered contrast-enhanced CCTA on a 64-slice GSI capable HDCT scanner (Discovery CT 750 High Definition, GE Healthcare) for clinical indication ( $n = 8$ ) or gave written informed consent to undergo CCTA for scientific purposes within the study protocol as approved by the ethics committee ( $n = 13$ ).

Exclusion criteria were known hypersensitivity to iodinated contrast agent, renal insufficiency (glomerular filtration rate  $< 60$  mL/min), and non-sinus rhythm.

### CCTA acquisition, reconstruction, and analysis

Patients who had a heart rate higher than 65 bpm received intravenous metoprolol (up to 25 mg Beloc, AstraZeneca, London, UK) prior to the examination to obtain optimal image quality for CCTA. To all patients, 2.5 mg isosorbiddinitrate (Isoket, Schwarz Pharma, Monheim, Germany) was administered sublingually prior to the scan. Iodixanol (Visipaque 320, 320 mg/mL, GE Healthcare, Buckinghamshire, UK) was injected into an antecubital vein followed by 50 mL saline solution via an 18-gauge catheter. Contrast media volume (40–95 mL) and flow rate (3.5–5 mL/s) were adapted to body surface area as previously validated.<sup>16</sup>

All scans were performed with prospective ECG triggering during inspiratory breath-hold at 75% of the R-R interval as previously reported.<sup>17–19</sup> The scans were acquired on a 64-slice HDCT that is able to switch the energy of the x-ray beam between 80 and 140 kVp within 0.3–0.5 ms during the scan and is complemented by a gemstone detector with very fast primary speed and low afterglow.<sup>20</sup>

The scanning protocol was adapted to individual body mass index (calculated as weight divided by square of height; kg/m<sup>2</sup>) using GSI presets as previously reported in detail.<sup>14</sup> In brief, tube current ranged from 375 to 640 mA, while GSI mode with fast tube voltage switching between 80 and 140 kVp on adjacent views during a single rotation resulted in a mean tube voltage ranging from 105 to 112 kV. The following scanning parameters were used in addition: axial scan mode with  $64 \times 0.625$  mm, gantry rotation time of 350 ms, and temporal resolution of 175 ms.

From the acquired data, conventional polychromatic images corresponding to the 140 kVp tube voltage as well as monochromatic image sets from the GSI data file (50, 60, 70, 80, 90, 100, 120, and 140 keV) were used.

All images were transferred to a dedicated workstation (AW 4.6, GE Healthcare) for analysis of stent geometry as well as attenuation measurements blinded to the results of the invasive coronary angiography and the stent's manufactures information. Luminal diameter was measured in oblique plane reconstructions along the course of the stents using a zoomed field of view with a fixed window level at 240 HU and window width of 1200 HU to ensure exact placement of the calipers. To assess the in-stent luminal diameter, three to six measurements were performed (one measurement approximately every 4–6 mm) by using electronic calipers. The stent length was not assessed because in serial stents with overlaps, stent edges would not be identifiable. To ensure that all measurements were performed in all the reconstructions

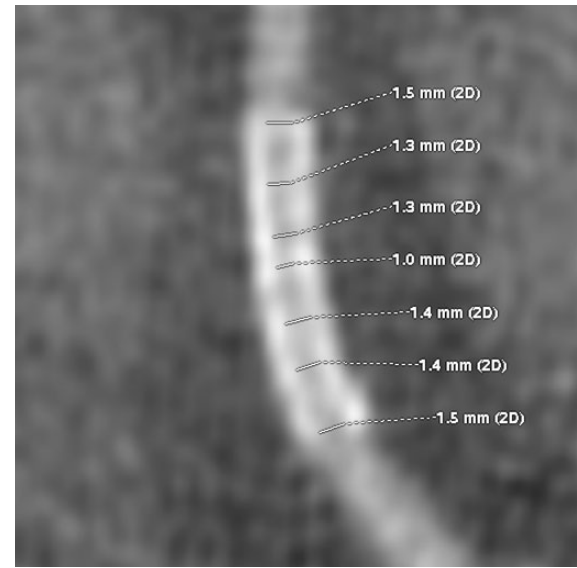


**Figure 1** Curved multi-planar reconstruction of CT coronary angiography images illustrating stent geometry measurements. To assess the in-stent luminal diameter, repeat measurements were performed ( $\sim 4$ – $6$  mm apart) by using electronic calipers, and the values were averaged.

at precisely the same location, we used two screens, whereby each monitor presented four panels, allowing the observer to view eight reconstructions simultaneously (Figure 1).

CT attenuation was assessed by measuring the mean signal value in Hounsfield Units (HU) and the noise in a region of interest (ROI) of  $1 \times 1$  mm placed in the stent lumen, carefully avoiding the lumen walls, stent struts, or streak artefacts, and in the ascending aorta. All ROIs were automatically projected in exactly the same location in all the reconstructions. Signal was defined as mean and noise as the standard deviation of the mean attenuation of the ROI.

Effective radiation dose from CCTA was calculated as the product of dose-length product (DLP) times a conversion coefficient for chest [ $k = 0.014$  mSv/(mGy cm)] as previously reported.<sup>21</sup>

### ICA acquisition and analysis

Angiograms of the target vessels were obtained in at least two orthogonal projections. The contrast-filled angiography catheter was used as reference for calibration. Stent diameter measurements on ICA were obtained blinded to the results from CCTA with a dedicated software (QCA analysis software, Xcelera, Philips Medical Systems, the Netherlands) in at least two views in the diastolic phase and then averaged. In the non-contrast-filled vessels, 2–12 measurements were performed (one measurement approximately every 2–4 mm) to assess in-stent luminal diameters as previously reported.<sup>22</sup>

### Statistical analysis

SPSS 22.0 (SPSS, Chicago, IL, USA) was used for all statistical analysis. Quantitative data were expressed as mean  $\pm$  standard deviation (SD) or median and inter-quartile range (IQR), when appropriate. The Kolmogorov–Smirnov test was applied to evaluate the distribution of the data. Comparison of continuous variables with non-normal distributions between groups was performed with the Wilcoxon signed-rank test

and with normal distribution with Student's paired *t*-test or Mann–Whitney *U* test. Comparison of attenuation measurements was performed with Mann–Whitney *U* test and conducted repeated-measures ANOVA testing. Friedman test and *post hoc* pairwise comparison were used for differences in stent diameter dependent on energy.

## Results

### Study population

CCTA and ICA were successfully performed in 21 patients (3 women, 18 men; mean age  $61 \pm 11.6$  years; range 43–84 years) with a total of 62 stents (range: 1–7 stents per patient) of whom 8 patients underwent ICA the same day and 13 patients within a mean of  $11.6 \pm 18.6$  days. The patient baseline characteristics are shown in Table 1.

After intravenous administration of  $13.6 \pm 7.2$  mg (range: 5–25 mg) beta blocker in 14 patients, the mean heart rate during scan acquisition was  $59.8 \pm 7.5$  bpm (range: 50–83).

### Radiation dose

Mean effective radiation dose was  $1.8 \pm 0.6$  mSv (DLP  $127.9 \pm 45.6$  mGy cm). The CT acquisition parameters are given in Table 2.

### Stent characteristics

There were 11 different types of stents implanted in the patients, e.g. Resolute Integrity ( $n = 32$ ), Cypher ( $n = 6$ ), Multi Link ( $n = 6$ ), Biomatrix ( $n = 5$ ), Biomatrix flex ( $n = 3$ ), Promus ( $n = 2$ ), Xcience ( $n = 2$ ), Taxus 3.0 ( $n = 2$ ), Taxus Express ( $n = 1$ ), Taxus Liberty ( $n = 1$ ), Skylor ( $n = 1$ ), and in one stent manufacture information was not available (Table 3). The stent size ranged from 2.25 to 5 mm (2.25 mm,  $n = 3$ ; 2.5 mm,  $n = 9$ ; 2.75 mm,  $n = 17$ ; 3 mm,  $n = 13$ ; 3.5 mm,  $n = 11$ ; 4 mm,  $n = 4$ ; 5 mm,  $n = 4$ ).

**Table 1 Patient baseline characteristics**

Number of patients	21
Age (years)	$61 \pm 11.6$ (43–84)
Male/female	18/3
BMI ( $\text{kg}/\text{m}^2$ )	$27.8 \pm 4.1$ (22.7–37.6)
Clinical symptoms	
Dyspnoea	4 (19)
Typical AP	8 (38)
Atypical chest pain	4 (19)
None	8 (38)
Cardiovascular risk factors	
Smoking	14 (67)
Diabetes	3 (14)
Arterial hypertension	13 (62)
Dyslipidaemia	16 (76)
Positive family history	8 (38)

Values are given as mean  $\pm$  SD and ranges (in brackets) or absolute numbers and percentages (in brackets); bpm, beats per minute; BMI, body mass index; AP, angina pectoris.

### Attenuation measurements

In-stent luminal attenuation was higher than aortic root attenuation in the polychromatic reconstruction ( $P < 0.001$ ), as well as throughout all the monochromatic reconstructions ( $P < 0.001$ ). Furthermore, an increase in monochromatic energy was associated with a decrease in the in-stent luminal attenuation and the aortic root attenuation (Figure 2;  $P < 0.001$ ).

**Table 2 CCTA acquisition parameters**

Beta blocker (mg)	$13.6 \pm 7.2$ (5–25)
Heart rate (bpm)	$59.8 \pm 7.5$ (50–83)
Contrast media volume (mL)	$72.9 \pm 15.9$ (40–95)
Contrast media flow (mL/s)	$4.5 \pm 0.5$ (3.5–5.0)
Effective radiation dose (mSv)	$1.8 \pm 0.6$ (1.2–3.6)

Values are given as mean  $\pm$  SD and ranges (in brackets); CCTA, coronary computed tomography angiography.

**Table 3 Stent characteristics**

Total number of stents	62
Stents per patient	$2.34 \pm 1.43$ (1–7)
In-stent restenosis	0
Stent localization	
LM	1 (2)
LAD	32 (52)
CX	9 (15)
RCA	17 (27)
IM	3 (5)
Device	
Resolute Integrity	32 (52)
Cypher	6 (10)
Multi Link	6 (10)
Biomatrix	5 (8)
Biomatrix flex	3 (5)
Promus	2 (3)
Xcience	2 (3)
Taxus 3.0	2 (3)
Taxus Express	1 (2)
Taxus Liberte	1 (2)
Skylor	1 (2)
Stent size (mm)	
2.25	3 (5)
2.5	9 (15)
2.75	17 (27)
3	13 (21)
3.5	11 (18)
4	4 (6)
5	4 (6)

Values are given as mean  $\pm$  SD and ranges (in brackets) or absolute numbers and percentages (in brackets). LM, left main; LAD, left anterior descending; CX, left circumflex artery; RCA, right coronary artery; Branches of LAD, CX, and RCA were attributed to the main artery. IM, intermediate artery.

At 80 keV or higher, the in-stent attenuation was lower in monochromatic than in polychromatic CCTA (Figure 3).

Stent geometry

Compared with QCA, mean in-stent luminal diameter was systematically underestimated with polychromatic (–39%) and each monochromatic

CCTA reconstruction. The largest underestimation (–90%) was found at the lowest monochromatic energy reconstruction (50 keV), which was substantially improved (–37% diameter underestimation) in high-energy monochromatic reconstruction (140 keV;  $P < 0.001$ ) (Table 4; Figure 4).

Discussion

This study reports the quantitative *in vivo* assessment of coronary artery stents with single-source, dual-energy CT allowing monochromatic image reconstruction, compared with QCA as standard of reference.

Our results suggest that low-energy, monochromatic reconstruction should not be used for coronary stent imaging, as this leads to a significant underestimation of in-stent luminal diameter of up to 90% compared with QCA. In contrast, monochromatic image reconstruction of 80 keV or higher allow reliable stent imaging, with stent attenuation and diameter values comparing well with those obtained with standard polychromatic CCTA.

Monochromatic image reconstruction was enabled by a new generation of single-source, dual-energy CT scanner, which allows multi-energy reconstruction by fast tube voltage switching. Recently, single-source, dual-energy scanning has been shown to offer significant noise reduction and image quality improvement in CCTA yielding optimal results using monochromatic reconstructions between 65 and 75 keV for coronary arteries without stents.<sup>14</sup>

The present results suggest the use of slightly higher monochromatic energy for stent imaging, i.e. 80 keV or higher. This finding is most probably due to the fact that attenuation from the stent material is substantially more pronounced than the iodine attenuation and causes beam hardening. The latter results in artificial underestimation

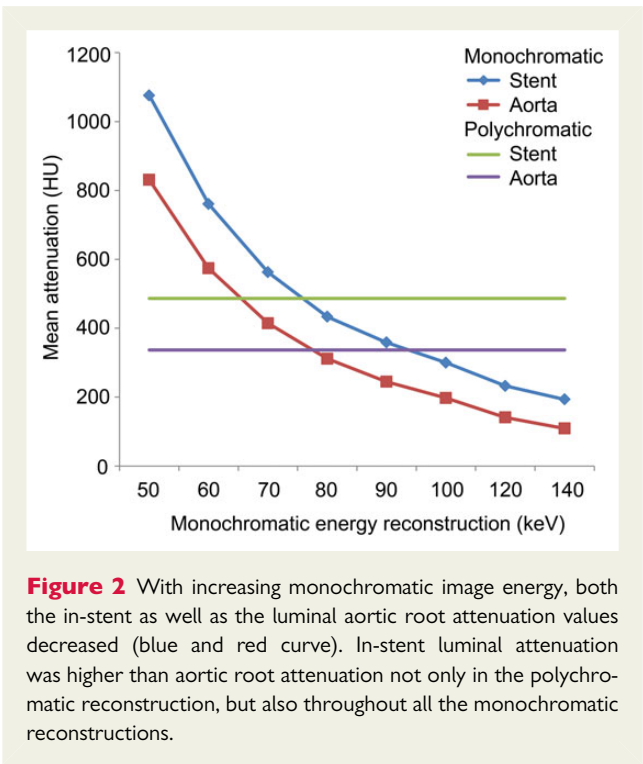


**Figure 2** With increasing monochromatic image energy, both the in-stent as well as the luminal aortic root attenuation values decreased (blue and red curve). In-stent luminal attenuation was higher than aortic root attenuation not only in the polychromatic reconstruction, but also throughout all the monochromatic reconstructions.

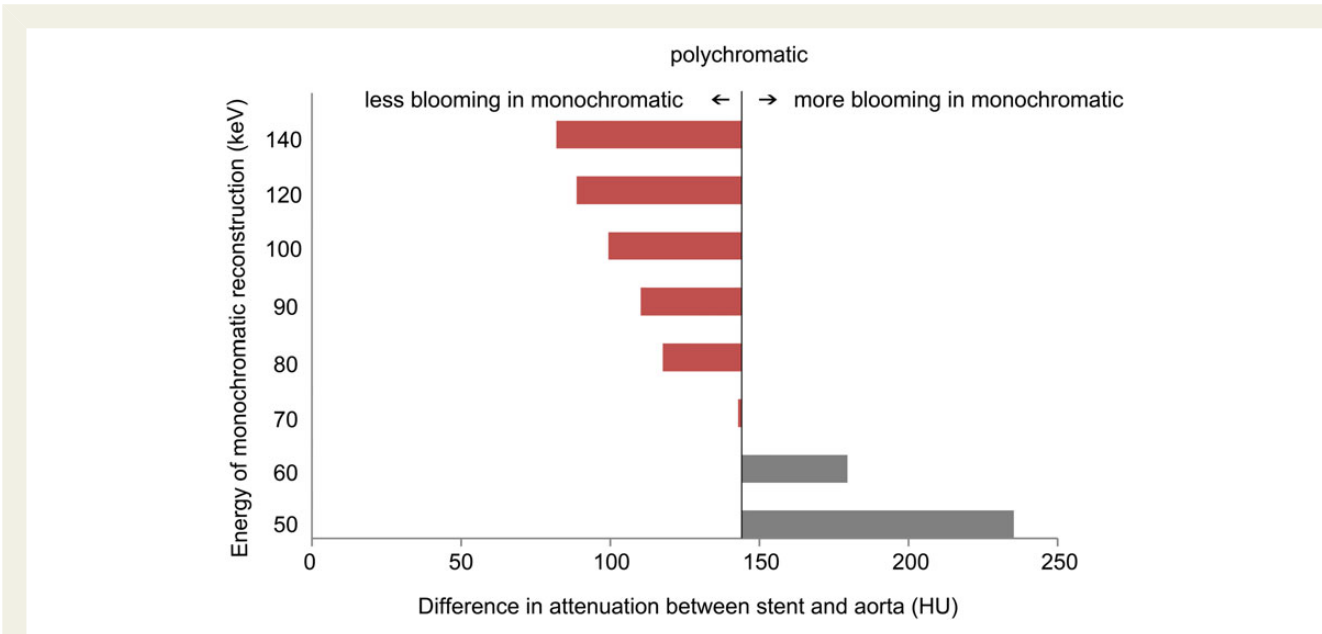


**Figure 3** At 80 keV and above, the difference in in-stent and aortic root attenuation was lower in monochromatic than in polychromatic CCTA, indicating that blooming within the stent was reduced in monochromatic CCTA at these energies. Below 70 keV, the blooming was more pronounced in monochromatic than in polychromatic CCTA.

**Table 4** In-stent luminal diameters of QCA versus polychromatic and monochromatic CCTA reconstructions

	QCA	Standard	50 keV	80 keV	140 keV
All stents (n = 62)					
Mean diameter (mm)	2.54 ± 0.72	1.55 ± 0.57	0.29 ± 0.40	1.55 ± 0.56	1.60 ± 0.57
Mean difference (%)	–	–38.6 ± 12.9	–89.7 ± 13.7	–38.7 ± 13.3	–36.6 ± 14.0
Stents ≥ 3 mm (n = 32)					
Mean diameter (mm)	2.92 ± 0.70	1.88 ± 0.56	0.40 ± 0.44	1.87 ± 0.56	1.90 ± 0.58
Mean difference (%)	–	–35.2 ± 11.6	–86.9 ± 13.0	–35.5 ± 12.4	–34.6 ± 12.2
Stents < 3 mm (n = 30)					
Mean diameter (mm)	2.13 ± 0.47	1.20 ± 0.30	0.17 ± 0.32	1.20 ± 0.31	1.28 ± 0.36
Mean difference (%)	–	–42.3 ± 13.4	–92.7 ± 13.9	–42.2 ± 13.7	–38.6 ± 15.7

Values are given as mean ± SD. QCA, quantitative coronary angiography. Standard means standard polychromatic reconstruction.

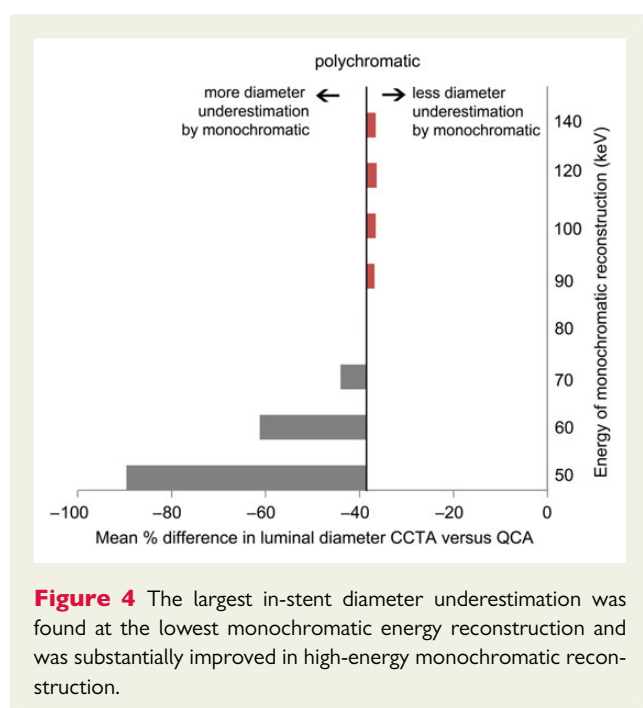


**Figure 4** The largest in-stent diameter underestimation was found at the lowest monochromatic energy reconstruction and was substantially improved in high-energy monochromatic reconstruction.

of the in-stent lumen in CCTA. Although multi-energy scanning may theoretically offer the potential of reducing beam hardening, our results suggest that the current technique does not yet reduce substantially the beam hardening compared with standard CCTA. In fact, luminal diameter underestimation was comparable in monochromatic vs. polychromatic CCTA. Therefore, this remains a fundamental limitation of coronary stent imaging by CCTA even in stents with a greater diameter than 3 mm. This has potentially critical clinical implications, as recent coronary revascularization guidelines recommend a follow-up CCTA for patients with unprotected left main stenting.<sup>11</sup> Although accurate stent lumen evaluation by CCTA remains a formidable task even in larger stents, and monochromatic CCTA does not appear to confer a substantial improvement, despite a slightly reduced blooming at higher energy reconstruction.

It may be perceived as a potential limitation of this study that 12 different types of stents were analysed in the present analysis. However,

the consistency of our results throughout several stent types further strengthens our observation. In addition, we did not exclude patients with heart rate > 65 bpm, although for CCTA with prospective ECG triggering optimal image quality can be expected below 65 bpm. In the present study, all patients were included regardless of heart rate to avoid a selection bias in favour of the evaluated technique. As only four patients had a heart rate ≥ 65 bpm, no meaningful subgroup analysis of these patients can be provided. Furthermore, all reconstructions were performed with conventional filtered back projection technique, although several modern iterative reconstruction algorithms have been introduced recently.<sup>23–27</sup> However, as the intention was to evaluate the impact of monochromatic imaging using different energy levels, we were cautious to maintain all other parameters unchanged to exclude confounders. Finally, no accuracy data are given, because the lack of any in-stent restenosis in the study population precluded calculation of meaningful accuracy parameters.

## Conclusions

Single-source, dual-energy scanning with monochromatic reconstruction can be used reliably for CCTA of coronary artery stents. However, reconstructions with energies below 80 keV are not recommended as the blooming artefacts are most pronounced at such low energies, resulting in up to 90% stent diameter underestimation.

## Acknowledgements

We thank Gentian Cermjani, Franziska Jann, and Ennio Mueller for their excellent technical support.

**Conflict of interest:** Institutional research grant from GE Healthcare.

## Funding

The study was supported by grants from the Swiss National Science Foundation to P.A.K.

## References

1. Buechel RR, Pazhenkottil AP, Herzog BA, Brueckner M, Nkoulou R, Ghadri JR et al. Prognostic performance of low-dose coronary CT angiography with prospective ECG triggering. *Heart* 2011;**97**:1385–90.

2. Chow BJ, Small G, Yam Y, Chen L, Achenbach S, Al-Mallah M et al. Incremental prognostic value of cardiac computed tomography in coronary artery disease using CONFIRM: COroNary computed tomography angiography evaluation for clinical outcomes: an International Multicenter registry. *Circ Cardiovasc Imaging* 2011;**4**: 463–72.
3. Kruger S, Mahnken AH, Sinha AM, Borghans A, Dedden K, Hoffmann R et al. Multislice spiral computed tomography for the detection of coronary stent restenosis and patency. *Int J Cardiol* 2003;**89**:167–72.
4. Maintz D, Juergens KU, Wichter T, Grude M, Heindel W, Fischbach R. Imaging of coronary artery stents using multislice computed tomography: in vitro evaluation. *Eur Radiol* 2003;**13**:830–5.
5. Schuijff JD, Bax JJ, Jukema JW, Lamb HJ, Warda HM, Vliegen HW et al. Feasibility of assessment of coronary stent patency using 16-slice computed tomography. *Am J Cardiol* 2004;**94**:427–30.
6. Zhang S, Levin DC, Halpern EJ, Fischman D, Savage M, Walinsky P. Accuracy of MDCT in assessing the degree of stenosis caused by calcified coronary artery plaques. *Am J Roentgenol* 2008;**191**:1676–83.
7. Andreini D, Pontone G, Bartorelli AL, Trabattoni D, Mushtaq S, Bertella E et al. Comparison of feasibility and diagnostic accuracy of 64-slice multidetector computed tomographic coronary angiography versus invasive coronary angiography versus intravascular ultrasound for evaluation of in-stent restenosis. *Am J Cardiol* 2009;**103**:1349–58.
8. Pflederer T, Marwan M, Renz A, Bachmann S, Ropers D, Kuettner A et al. Non-invasive assessment of coronary in-stent restenosis by dual-source computed tomography. *Am J Cardiol* 2009;**103**:812–7.
9. Kumbhani DJ, Ingelmo CP, Schoenhagen P, Curtin RJ, Flamm SD, Desai MY. Meta-analysis of diagnostic efficacy of 64-slice computed tomography in the evaluation of coronary in-stent restenosis. *Am J Cardiol* 2009;**103**:1675–81.
10. Gogas BD, Garcia-Garcia HM, Onuma Y, Muramatsu T, Farooq V, Bourantas CV et al. Edge vascular response after percutaneous coronary intervention: an intracoronary ultrasound and optical coherence tomography appraisal: from radioactive platforms to first- and second-generation drug-eluting stents and bioresorbable scaffolds. *JACC Cardiovasc Interv* 2013;**6**:211–21.
11. Task Force on Myocardial Revascularization of the European Society of Cardiology, the European Association for Cardio-Thoracic Surgery, European Association for Percutaneous Cardiovascular Interventions, Wijns W, Kolh P, Danchin N et al. Guidelines on myocardial revascularization. *Eur Heart J* 2010;**31**:2501–55.
12. Zhang D, Li X, Liu B. Objective characterization of GE discovery CT750 HD scanner: gemstone spectral imaging mode. *Med Phys* 2011;**38**:1178–88.
13. Karcaaltincaba M, Aktas A. Dual-energy CT revisited with multidetector CT: review of principles and clinical applications. *Diagn Interv Radiol* 2011;**17**:181–94.
14. Fuchs TA, Stehli J, Fiechter M, Dougoud S, Gebhard C, Ghadri JR et al. First experience with monochromatic coronary computed tomography angiography from a 64-slice CT scanner with Gemstone Spectral Imaging (GSI). *J Cardiovasc Comput Tomogr* 2013;**7**:25–31.
15. Fuchs TA, Sah BR, Stehli J, Bull S, Dougoud S, Huellner MW et al. Attenuation correction maps for SPECT myocardial perfusion imaging from contrast-enhanced coronary CT angiography: gemstone spectral imaging with single-source dual energy and material decomposition. *J Nucl Med* 2013;**54**:2077–80.
16. Pazhenkottil AP, Husmann L, Buechel RR, Herzog BA, Nkoulou R, Burger IA et al. Validation of a new contrast material protocol adapted to body surface area for optimized low-dose CT coronary angiography with prospective ECG-triggering. *Int J Cardiovasc Imaging* 2010;**26**:591–7.
17. Husmann L, Valenta I, Gaemperli O, Adda O, Treyer V, Wyss CA et al. Feasibility of low-dose coronary CT angiography: first experience with prospective ECG-gating. *Eur Heart J* 2008;**29**:191–7.
18. Herzog BA, Husmann L, Burkhard N, Gaemperli O, Valenta I, Tatsugami F et al. Accuracy of low-dose computed tomography coronary angiography using prospective electrocardiogram-triggering: first clinical experience. *Eur Heart J* 2008;**29**:3037–42.
19. Buechel RR, Husmann L, Herzog BA, Pazhenkottil AP, Nkoulou R, Ghadri JR et al. Low-dose computed tomography coronary angiography with prospective electrocardiogram triggering: feasibility in a large population. *J Am Coll Cardiol* 2011;**57**: 332–6.
20. Lin XZ, Miao F, Li JY, Dong HP, Shen Y, Chen KM. High-definition CT Gemstone spectral imaging of the brain: initial results of selecting optimal monochromatic image for beam-hardening artifacts and image noise reduction. *J Comput Assist Tomogr* 2011;**35**:294–7.
21. Hausleiter J, Meyer T, Hermann F, Hadamitzky M, Krebs M, Gerber TC et al. Estimated radiation dose associated with cardiac CT angiography. *JAMA* 2009;**301**: 500–7.
22. Schepis T, Koepfli P, Leschka S, Desbiolles L, Husmann L, Gaemperli O et al. Coronary artery stent geometry and in-stent contrast attenuation with 64-slice computed tomography. *Eur Radiol* 2007;**17**:1464–73.
23. Leipsic J, Labounty TM, Heilbron B, Min JK, Mancini GB, Lin FY et al. Adaptive statistical iterative reconstruction: assessment of image noise and image quality in coronary CT angiography. *Am J Roentgenol* 2010;**195**:649–54.
24. Utsunomiya D, Weigold WG, Weissman G, Taylor AJ. Effect of hybrid iterative reconstruction technique on quantitative and qualitative image analysis at 256-slice prospective gating cardiac CT. *Eur Radiol* 2012;**22**:1287–94.
25. Schuhbaeck A, Achenbach S, Layritz C, Eisentopf J, Hecker F, Pflederer T et al. Image quality of ultra-low radiation exposure coronary CT angiography with an effective dose <0.1 mSv using high-pitch spiral acquisition and raw data-based iterative reconstruction. *Eur Radiol* 2013;**23**:597–606.
26. Yoo RE, Park EA, Lee W, Shim H, Kim YK, Chung JW et al. Image quality of Adaptive Iterative Dose Reduction 3D of coronary CT angiography of 640-slice CT: comparison with filtered back-projection. *Int J Cardiovasc Imaging* 2013;**29**:669–76.
27. Fuchs TA, Fiechter M, Gebhard C, Stehli J, Ghadri JR, Kazakauskaitė E et al. CT coronary angiography: impact of adapted statistical iterative reconstruction (ASIR) on coronary stenosis and plaque composition analysis. *Int J Cardiovasc Imaging* 2013;**29**:719–24.